Published in final edited form as:
Arterioscler Thromb Vasc Biol. 2012 August ; 32(8): 1817–1823. doi:10.1161/ATVBAHA.112.247262.

Genetic ablation of *Adamts13* gene dramatically accelerates the formation of early atherosclerosis in a murine model

Junichiro Tohyama[2,†], **Robert C. Bauer**[2], **Na Nora Cao**[1], **Daniel J. Rader**[2,3], and **X. Long Zheng**[1,3]

[1]Department of Pathology and Laboratory Medicine, The Children's Hospital of Philadelphia, Philadelphia, PA 19104

[2]Department of Medicine, Hospital of the University of Pennsylvania, Philadelphia, PA 19104

[3]The University of Pennsylvania Perelman School of Medicine, Philadelphia, PA 19104

Abstract

Objective—ADAMTS13 cleaves von Willebrand factor (VWF), thereby modulating thrombosis and inflammation. Low plasma ADAMTS13 activity is associated with cardiovascular events including myocardial and cerebral infarction. Here, we investigated the role of ADAMTS13 in the development of early atherosclerosis in a murine model.

Methods and Results—*ApoE*$^{-/-}$ and *Adamts13*$^{-/-}$*ApoE*$^{-/-}$ mice were fed with a high fat Western diet for 12 weeks. Atherosclerotic lesions in the aorta and aortic roots were quantified after staining. Leukocyte rolling and adhesion onto cremaster venules after oxidative injury were determined by intravital microscopy. While plasma cholesterol levels were largely similar in both groups, the extent of atherosclerotic lesions in the aorta *en face* and in the aortic roots in the *Adamts13*$^{-/-}$*ApoE*$^{-/-}$ mice increased ~5.5 fold (p=0.0017) and ~6.1 fold (p=0.0037), respectively. Also, the ratio of plasma high to low molecular weight VWF multimers increased ~3 fold. The leukocyte rolling velocities were significantly reduced (p<0.001) with an increased number of leukocyte rolling (p=0.0026) and macrophage infiltration into the atherosclerotic lesions in the *Adamts13*$^{-/-}$*ApoE*$^{-/-}$ mice.

Conclusions—Our results suggest that ADAMTS13 plays a critical role in modulating the development of early atherosclerosis, likely through proteolytic cleavage of ultra large VWF multimers, thereby inhibiting platelet deposition and inflammation.

Keywords

von Willebrand factor cleaving protease; inflammation; and animal model

Introduction

ADAMTS13, a member of *A*Disintegrin *A*nd *M*etalloprotease with *T*hrombo*S*pondin type 1 repeats family, is primarily synthesized in the liver [1, 2]. Plasma ADAMTS13 metalloprotease cleaves a blood adhesion protein von Willebrand factor (VWF) at the Tyr^{1605}-Met^{1606} bond [3, 4]. VWF is synthesized in all vascular endothelial beds and

Correspondence should be addressed to: X. Long Zheng Department of Pathology and Laboratory Medicine The Children's Hospital of Philadelphia The 34th Street and Civic Center Blvd, 816G ARC, Philadelphia, PA 19104, U.S.A.
†These authors contribute equally to this work.

Disclosures
The authors have no relevant conflict of interest to disclose.

constitutively secreted or stored in Weibel-Palade bodies of the endothelium [5]. Upon stimulation by a variety of agonists such as epinephrine [6], ADP [7], and thrombin [8] or desmopressin [9], the stored VWF multimers are released. The newly released ultra large (UL) VWF forms "string-like" polymers, which remain anchored on endothelial cell membrane. The cell bound VWF polymers are highly sensitive to proteolysis by plasma ADAMTS13 metalloprotease [10–12]. Once being released into circulation, VWF polymers alter their conformations, becoming resistant to ADAMTS13 until they are unfolded by arterial shear stress [13, 14]. If this process is compromised, ultra large VWF polymers bind circulating platelets spontaneously and cause exaggerated platelet aggregation and disseminated thromboses in small arteries and capillaries, exemplified by thrombotic thrombocytopenic purpura (TTP), a potentially fatal syndrome [14–16].

ADAMTS13 and VWF play an opposite role in thrombosis and systemic inflammation. *Adamts13*$^{-/-}$ mice exhibit an increase in leukocyte rolling, adhesion, and extravasation in a murine model of acute inflammation [17]. Epidemiological studies also show an association between the reduced ratio of plasma ADAMTS13 activity to VWF antigen and pathological conditions such as chronic inflammation [18] and cardiovascular [19] or cerebral vascular events [20].

Here, we demonstrate that genetic ablation of the *Adamts13* gene in the *ApoE*-null mice (*Adamts13*$^{-/-}$ *ApoE*$^{-/-}$) fed a high fat Western diet dramatically accelerates the development of early atherosclerosis. Also, an increased leukocyte rolling over endothelium after oxidative injury and increased macrophage infiltration into atherosclerotic lesions may underlie the pathogenesis of atherosclerosis in *Adamts13*$^{-/-}$*ApoE*$^{-/-}$ mice. Together, our findings demonstrate the critical role of ADAMTS13 proteolysis in modulating early atherosclerosis in genetically susceptible mice.

Methods

Animals and diet

All animal studies were approved by Institutional Animal Care and Use Committees (IACUC) at The Children's Hospital of Philadelphia and The University of Pennsylvania Perelman School of Medicine. *ApoE*$^{-/-}$ mice (C57BL/6J strain) were purchased from the Jackson Laboratory (Bar Harbor, Maine). *Adamts13*$^{-/-}$ mice (C57BL/6/129 strain) were kindly provided by Dr. David Ginsburg (Department of Internal Medicine, University of Michigan, Ann Arbor, Michigan). *ApoE*$^{-/-}$ and *Adamts13*$^{-/-}$ mice were bred for more than four times to generate *Adamts13*$^{-/-}$ *ApoE*$^{-/-}$ mice. Mice at the age of 6 weeks were fed with a high fat Western diet from Harlan Laboratories (Madison, Wisconsin) consisting of 21.2% fat and 0.2% cholesterol for a total of 12 weeks.

Blood collection

Whole blood (200 μl) was collected via retro orbital sinus plexus from mice after 4 hours of fasting for plasma lipid analyses. The blood was anti-coagulated (9:1, vol:vol) with 3.9% sodium citrate. Plasma was obtained after centrifugation for 10 min at 10,000 rpm in a microcentrifuge and stored in aliquots at −80 °C.

En face Oil red staining of atherosclerotic lesions in aorta

Mice were euthanized by intra-peritoneal injection of a lethal dose of nembutal. The entire aorta and heart were surgically isolated under a dissecting microscope and fixed overnight with 10% neutrally buffered formalin. The extent of atherosclerotic lesions *en face* in the aorta was determined by Oil Red O staining [21]. All images were obtained under a light

microscope with magnifications (100x and 200x) and quantified by ImageJ analysis software.

Histological examination of atherosclerotic lesions in aortic roots

The heart was fixed overnight with 10% neutral buffered formalin and embedded with tissue freezing medium (Ted Pella Inc, Redding California). The heart was then sectioned (6 μm, interspaced by 80 μm) using a cryostat. Twelve tissue sections from each heart were placed on each slide and stained with hematoxylin and eosin in the histology core facility at the University of Pennsylvania. Digital images were obtained for each section using a Nikon ECLIPSE-80i microscope equipped with a Nikon digital camera DXM1200. The areas of atherosclerotic lesions in all sections of entire aortic roots were analyzed with ImageJ software in a blind fashion.

Plasma VWF multimer analysis

Citrated mouse plasma (1.0 μL) was denatured by heating at 60°C for 20 minutes in 70 mM Tris-HCl, pH 6.5 containing 2.4% SDS, 4% urea, and 4 mM EDTA. The denatured sample was fractionated on a 1.0% SeaKem HGT agarose (Cambrex, East Rutherford, New Jersey) mini-gel by electrophoresis at 15 mA for 2.5 hours. After being transferred onto a nitrocellulose membrane (Bio-Rad, Hercules, California), the membrane was blocked by TBSc (20 mM Tris-HCl, pH 7.5,150 mM NaCl, and 1% casein) for 30 minutes. The membrane was incubated overnight at 4°C with rabbit anti-VWF IgG (DAKO, Carpinteria, California) in TBSc (1:1,500), followed by an incubation with IRDyeCW800-labeled goat anti–rabbit IgG (LI-COR, Lincoln, Nebraska) in TBSc (1:12,500) for 1 hour. The fluorescent signal was obtained using an Odyssey imaging system (LI-COR, Lincoln, Nebraska).

Lipid Analysis

Plasma total cholesterol, high-density lipoprotein (HDL) cholesterol, and triglyceride levels were determined on a chemistry analyzer (Roche Diagnostics Systems, Indianapolis, Indiana) using commercially available reagents (Wako Pure Chemical Industries and Trinity Biotech, Jamestown, New York).

Leukocyte rolling and velocity rate

Mice were anesthetized with an intra peritoneal injection of Nembutal. Cremaster vessels were exposed and injured by topical application of a filter paper soaked with 2.5% $FeCl_3$ for 10 sec. Rhodamine 6G (Sigma, St. Louis, Missouri) (1 μg/g body weight diluted with 100 μl of PBS) was injected via retro orbital sinus plexus to label leukocytes and platelets. The leukocytes rolling over the injured vessels were recorded in real time under an inverted fluorescent microscope (100x) equipped with a high-speed digital camera (Olympics, Center Valley, Pennsylvania). All movies were recorded using the NIS Elements software from Nikon Instruments, Inc (Melville, New York).

The number of leukocyte rolling and rolling velocity (μm/second) were determined offline using the NIS Elements image analysis program. The number of leukocytes rolling over the injured vessel was determined at 6 different sites in each mouse for a total 6 mice in each group. The velocity was determined by the equation (1):

$$v = \text{A fixed distance of } 100\,\mu\text{m} / \text{the required for traveling (seconds)} \quad (1)$$

Here, v refers to the velocity (μm/second).

The cumulative frequencies as a function of various velocities were fit into a sigmoidal curve using the GraphPad software (La Jolla, California).

Immunohistochemical staining of macrophages

After being embedded into tissue freezing medium, formalin-fixed aortic tissues were sectioned (6 μm) using a cryostat. Tissue sections were rinsed with PBS and treated with 0.1 M sodium citrate (pH 6.0) for 5 min in a pressure cooker to retrieve antigen. After being blocked with avidin-biotin blocking solution (Vector, Burlingame, California), the tissue sections were incubated overnight at 4°C with rat anti-mouse CD107b (Mac3) (BD Pargmingen, San Jose, California) (1:100) followed by incubation for one hour with ImmPRESS anti-rat IgG (Vector). The tissue sections were counterstained with hematoxylin and mounted with Permount medium purchased from Fisher Scientific (Pittsburgh, Pennsylvania). Digital images were obtained under a Nikon Eclipse 80i fluorescent microscope.

Statistical analysis

The means and standard deviation or standard error of the means (SEM) were determined. The difference of the continuous variances between two groups was determined by the two-tailed Student's *t*-test. One-way ANOVA analysis of the variants was determined with Prism5 GraphPad Software for the significant differences among various groups.

Results

Adamts13$^{-/-}$*ApoE*$^{-/-}$ mice show an increased formation of atherosclerotic lesions in aorta and aortic roots

Epidemiological studies suggest that a reduced ratio of plasma ADAMTS13 activity to plasma VWF antigen is a risk factor for development of cardiovascular diseases, particularly myocardial infarction [19, 22, 23] and ischemic stroke [20, 24]. However, the causative role of the reduced plasma ADAMTS13 activity and elevated plasma VWF has not been fully established. To address this question, *Adamts13*$^{-/-}$ ApoE$^{-/-}$ and *ApoE*$^{-/-}$ mice at the age of 6 weeks were fed a high fat Western diet for 12 weeks and then sacrificed. The entire aorta was isolated, fixed, and stained *en face* with oil red O. The results showed substantially greater lesion development in *Adamts13*$^{-/-}$ApoE$^{-/-}$ mice (Fig. 1B) as compared with that in *ApoE*$^{-/-}$ mice (Fig. 1A). Histological examination after hematoxylin and eosin (H&E) staining confirmed the atherosclerotic lesion in both groups of mice (Fig. 1C and 1D). Image analyses demonstrated that the relative surface areas of atherosclerotic plaques in the aortas of the *Adamts13*$^{-/-}$ ApoE$^{-/-}$ mice increased ~5.5 fold (p=0.00165) (Fig. 1E). Moreover, the hearts were harvested, embedded, and cryosectioned. The heart sections were stained with H&E, revealing substantially greater lesion development in the *Adamts13*$^{-/-}$ApoE$^{-/-}$ mice (Fig. 2B) than in the *ApoE*$^{-/-}$ mice (Fig. 2A). Image analyses further showed that the extent of atherosclerotic lesions in the aortic roots in the *Adamts13*$^{-/-}$ ApoE$^{-/-}$ mice increased ~6.1 fold (Fig. 2C) (p=0.00367). These results demonstrate that ADAMTS13 metalloprotease may play a critical role protecting against the formation of early atherosclerosis in genetically susceptible mice.

Ultra large VWF multimers are present in *Adamts13*$^{-/-}$*ApoE*$^{-/-}$ mice

Mice deficient for plasma ADAMTS13 activity show an accumulation of ultra large VWF multimers on stimulated or damaged endothelial cells [25] and in plasma [26, 27]. To determine whether *ApoE* deficiency plus being fed with a Western diet further impair VWF homeostasis, we determined plasma VWF multimer distribution by agarose gel electrophoresis as described in the Methods. The ratio of ultra large VWF to low molecular

weight VWF multimers in the *Adamts13*$^{-/-}$ *ApoE*$^{-/-}$ increased by ~3 fold compared with that in the *ApoE*$^{-/-}$ or wild-type mice (Fig. 3A and 3B). However, the ratio of ultra large VWF to low molecular weight VWF in these mice was not significantly different from that in the *Adamts13*$^{-/-}$ mice (Fig. 3). These results demonstrate that genetic ablation of *Adamts13* gene results in an accumulation of ultra large VWF multimers in plasma, but the additional deletion of the *ApoE* plus a high fat diet has no further deleterious effect on VWF homeostasis.

Adamts13 deficiency has little effect on plasma cholesterol metabolism

To rule out the potential effect of Adamts13 proteolysis on cholesterol metabolism, we determined plasma total cholesterol, HDLs, and triglycerides in various groups of mice after being fed a high fat Western diet for 12 weeks. The levels of total cholesterol, non-HDL cholesterol, and triglycerides did not significantly differ between *Adamts13*$^{-/-}$*ApoE*$^{-/-}$ mice and *ApoE*$^{-/-}$ mice, while the levels of HDL cholesterol in *Adamts13*$^{-/-}$*ApoE*$^{-/-}$ mice (95.3 ± 39.0 mg/dl) were slightly higher than in *ApoE*$^{-/-}$ mice (65.6 ± 17.4 mg/dl). The difference was statistically highly significant (p=0.02) (Table 1). The similar lipid profiles in both groups except for an increased level of HDL cholesterol in *Adamts13*$^{-/-}$ *ApoE*$^{-/-}$ mice suggest that the increase of atherosclerotic plagues is not the result of impaired cholesterol metabolism, but the direct effect of lacking ADAMTS13 metalloprotease.

Increased leukocyte rolling, adhesion, and infiltration in the *Adamts13*$^{-/-}$ *ApoE*$^{-/-}$ mice

VWF is the only known substrate of ADAMTS13 identified to date. Previous studies show that *Adamts13*$^{-/-}$ mice have enhanced systemic inflammatory responses, exhibiting increased leukocyte rolling, adhesion and extravasation, which depends on VWF [17]. By intravital microscopy, we showed that the number of fluorescent rhodamine 6G-labeled leukocytes rolling over or adhered to the injured venules was significantly increased in *Adamts13*$^{-/-}$*ApoE*$^{-/-}$ mice (44.1 ± 1.5, means ± SEM, n=6) compared with that in *ApoE*$^{-/-}$ mice (24.7 ± 0.8, means ± SEM, n=6) (p=0.0026) (Fig. 4). Consistently, the velocity of leukocyte rolling in the same vessels in the *Adamts13*$^{-/-}$*ApoE*$^{-/-}$ mice was dramatically reduced (p<0.001) (Fig. 4). These findings were mirrored by the increased number of infiltrated macrophages (Mac-3 positive) in the atherosclerotic plagues in the *Adamts13*$^{-/-}$*ApoE*$^{-/-}$ mice (Fig. 5). Together, these results indicate that ADAMTS13 metalloprotease plays an important role in attenuating systemic inflammatory responses.

Discussion

In the present study, we demonstrate that Adamts13$^{-/-}$ ApoE$^{-/-}$ mice develop more extensive and larger atherosclerotic plaques in the branch points of the aorta (Fig. 1) and the aortic roots (Fig. 2) after 12 weeks on a high fat Western diet. These results *suggest that ADAMTS13 metalloprotease protects against the development of early atherosclerosis in a genetically susceptible animal. Interestingly, the increase in atherosclerotic lesions in both the aorta and aortic arches in the Adamts13*$^{-/-}$ ApoE$^{-/-}$ mice appears to be much greater than that recently reported [28]. This discrepancy is not simply caused by the relatively low volume of atherosclerotic lesions in our control mice, as the area of atherosclerotic lesions in *ApoE*$^{-/-}$ mice (Fig. 1 and Fig. 2) from both studies is comparable [28]. While total cholesterols, triglycerides, and LDLs are not significantly altered, plasma HDL levels are significantly increased in *Adamts13*$^{-/-}$ ApoE$^{-/-}$ mice in this study (p=0.02). The mechanism underlying the HDL elevation in *Adamts13*$^{-/-}$ ApoE$^{-/-}$ mice is yet to be determined.

It is also not clear how ADAMTS13 metalloprotease protects against the formation of early atherosclerosis in *ApoE*$^{-/-}$ mice. We hypothesize that the deficiency of plasma ADAMTS13 activity results in an accumulation of ultra large VWF multimers on endothelial cell surfaces

and in plasma, which enhances both platelet aggregation and systemic inflammation. This hypothesis is based on a number of published studies showing the accumulation of ultra large VWF strings on endothelial cells upon injury in *Adamts13*$^{-/-}$ mice [17, 25, 29]. An infusion of recombinant ADAMTS13 rapidly eliminates the cell bound VWF strings *in vivo* [25, 29]. We showed that the ratio of plasma ultra large VWF to low molecular weight VWF multimers in either *Adamts13*$^{-/-}$ mice [26] or *Adamts13*$^{-/-}$ ApoE$^{-/-}$ mice were dramatically increased (Fig. 3). Both ultra large VWF multimers and adherent platelets have been shown to promote systemic and local inflammation, and play a role in the development of atherosclerosis [30, 31]. Consistent with this notion, the number of leukocytes rolled over the injured vessels increases ~2 fold, corresponding *with the significant reduction in leukocyte rolling velocity (*Fig. 4), which results in increased macrophage infiltration into the atherosclerotic lesions (Fig. 5). Similar findings have recently been reported at the site of atherosclerotic plagues in the carotid artery[32]. Together, these data suggest that an increased inflammatory response in Adamts13$^{-/-}$ ApoE$^{-/-}$ mice may contribute to the accelerated formation of atherosclerosis.

It remains to be determined, however, whether ADAMTS13 has a direct effect against atherosclerosis or merely functions to reduce the adhesiveness of ultra large VWF multimers, thereby an anti-athero effect is indirect. A previous study demonstrated a ~40% reduction of atherosclerotic lesion area in the *vwf*$^{-/-}$ and *LDLR*$^{-/-}$ mice compared with the *LDLR*$^{-/-}$ mice after 8 weeks on a high fat diet [33]. Furthermore, an inhibition of platelet adhesion to VWF with a monoclonal antibody against GP1bα also reduced leukocyte adhesion and formation of atherosclerotic lesions in the *ApoE*$^{-/-}$ mice [34]. These results support that VWF, platelets, and leukocytes all play a role in the development of early atherosclerosis.

The interaction between VWF and leukocytes is largely mediated by binding of endothelial VWF to leukocyte P-selectin glycoprotein ligand-1 (PSGL-1) [35, 36], P-selectin, and L-selectin [37, 38]. *PSGL-1*$^{-/-}$ mice exhibit selective impairment in leukocyte recruitment into the atherosclerotic arterial wall [39]. Inhibition of P-selectin completely abrogates leukocyte rolling in *Adamts13*$^{-/-}$ mice, suggesting that P-selectin is required for initiating leukocyte rolling even in the presence of endothelial VWF strings [17].

In conclusion, we demonstrate that the genetic ablation of the *Adamts13* gene in *ApoE* null mice fed a high diet results in an accelerated formation of early atherosclerosis. We hypothesize that the underlying mechanism may be associated with increased systemic and local inflammation as reflected by increased initial leukocyte rolling, adhesion, and infiltration at the site of injury. Our findings provide further evidence demonstrating the critical role of ADAMTS13 metalloprotease in attenuating the formation of early atherosclerotic plagues in a genetically susceptible individual.

Supplementary Material

Refer to Web version on PubMed Central for supplementary material.

Acknowledgments

The authors thank Dr. David Ginsburg from The Department of Genetics, University of Michigan, Ann Arbor, for providing *Adamts13*$^{-/-}$ mice.

Sources of Funding

This study is partially supported by grants from the American Heart Association Established Investigator Award (AHA-0940100N) and National Institute of Health (P01HL074124, project 3).

Reference List

1. Uemura M, Tatsumi K, Matsumoto M, Fujimoto M, Matsuyama T, Ishikawa M, Iwamoto TA, Mori T, Wanaka A, Fukui H, Fujimura Y. Localization of ADAMTS13 to the stellate cells of human liver. Blood. 2005; 106:922–924. [PubMed: 15855280]
2. Zheng XL, Chung D, Takayama T, Majerus E, Sadler J, Fujikawa K. Structure of von Willebrand factor-cleaving protease (ADAMTS13), a metalloprotease involved in thrombotic thrombocytopenic purpura. J Biol Chem. 2001; 276:41059–41063. [PubMed: 11557746]
3. Tsai HM. Physiologic cleavage of von Willebrand factor by a plasma protease is dependent on its conformation and requires calcium ion. Blood. 1996; 87:42354244.
4. Zheng XL, Majerus E, Sadler J. ADAMTS13 and TTP. Curr Opin Hematol. 2002; 9:389–394. [PubMed: 12172456]
5. Wagner DD, Marder VJ. Biosynthesis of von Willebrand protein by human endothelial cells: processing steps and their intracellular localization. J Cell Biol. 1984; 99:2123–2130. [PubMed: 6334089]
6. Goto S, Ikeda Y, Murata M, Handa M, Takahashi E, Yoshioka A, Fujimura Y, Fukuyama M, Handa S, Ogawa S. Epinephrine augments von Willebrand factor-dependent shear-induced platelet aggregation. Circulation. 1992; 86:1859–1863. [PubMed: 1360339]
7. Palmer DS, Aye MT, Ganz PR, Halpenny M, Hashemi S. Adenosine nucleotides and serotonin stimulate von Willebrand factor release from cultured human endothelial cells. Thromb Haemost. 1994; 72:132–139. [PubMed: 7974361]
8. Mayadas T, Wagner DD, Simpson PJ. von Willebrand factor biosynthesis and partitioning between constitutive and regulated pathways of secretion after thrombin stimulation. Blood. 1989; 73:706–711. [PubMed: 2783866]
9. Kaufmann JE, Oksche A, Wollheim CB, Gunther G, Rosenthal W, Vischer UM. Vasopressin-induced von Willebrand factor secretion from endothelial cells involves V2 receptors and cAMP. J Clin Invest. 2000; 106:107–116. [PubMed: 10880054]
10. Dong JF, Moake JL, Nolasco L, Bernardo A, Arceneaux W, Shrimpton CN, Schade AJ, McIntire LV, Fujikawa K, Lopez JA. ADAMTS-13 rapidly cleaves newly secreted ultralarge von Willebrand factor multimers on the endothelial surface under flowing conditions. Blood. 2002; 100:4033–4039. [PubMed: 12393397]
11. Dong JF, Moake JL, Bernardo A, Fujikawa K, Ball C, Nolasco L, Lopez JA, Cruz MA. ADAMTS-13 metalloprotease interacts with the endothelial cell-derived ultra-large von Willebrand factor. J Biol Chem. 2003; 278:29633–19639. [PubMed: 12775718]
12. Dong JF. Cleavage of ultra-large von Willebrand factor by ADAMTS-13 under flow conditions. J Thromb Haemost. 2005; 3:1710–1716. [PubMed: 16102037]
13. Tsai HM, Sussman I, Nagel RL. Shear stress enhances the proteolysis of von Willebrand factor in normal plasma. Blood. 1994; 83:2171–2179. [PubMed: 8161783]
14. Tsai HM, Lian EC. Antibodies to von Willebrand factor-cleaving protease in acute thrombotic thrombocytopenic purpura. N Engl J Med. 1998; 339:1585–1594. [PubMed: 9828246]
15. Moake JL. Thrombotic microangiopathies. N Engl J Med. 2002; 347:589–600. [PubMed: 12192020]
16. Zheng XL, Pallera AM, Goodnough LT, Sadler JE, Blinder MA. Remission of chronic thrombotic thrombocytopenic purpura after treatment with cyclophosphamide and rituximab. Ann Intern Med. 2003; 138:105–108. [PubMed: 12529092]
17. Chauhan AK, Kisucka J, Brill A, Walsh MT, Scheiflinger F, Wagner DD. ADAMTS13: a new link between thrombosis and inflammation. J Exp Med. 2008; 205:2065–2074. [PubMed: 18695007]
18. Reiter R, Varadi K, Turecek P, Jilma B, Knobl P. Changes in ADAMTS13 (von- Willebrand-factor-cleaving protease) activity after induced release of von Willebrand factor during acute systemic inflammation. Thromb Haemost. 2005; 93:554–558. [PubMed: 15735809]
19. Matsukawa M, Kaikita K, Soejima K, Fuchigami S, Nakamura Y, Honda T, Tsujita K, Nagayoshi Y, Kojima S, Shimomura H, Sugiyama S, Fujimoto K, Yoshimura M, Nakagaki T, Ogawa H. Serial changes in von Willebrand factor-cleaving protease (ADAMTS13) and prognosis after acute myocardial infarction. Am J Cardiol. 2007; 100:758–763. [PubMed: 17719316]

20. Bongers TN, De Maat MP, van Goor ML, Bhagwanbali V, van Vliet HH, Gomez Garcia EB, Dippel DW, Leebeek FW. High von Willebrand factor levels increase the risk of first ischemic stroke: influence of ADAMTS13, inflammation, and genetic variability. Stroke. 2006; 37:2672–2677. [PubMed: 16990571]
21. Tangirala RK, Tsukamoto K, Chun SH, Usher D, Pure E, Rader DJ. Regression of atherosclerosis induced by liver-directed gene transfer of apolipoprotein A-I in mice. Circulation. 1999; 100:1816–1822. [PubMed: 10534470]
22. Kaikita K, Soejima K, Matsukawa M, Nakagaki T, Ogawa H. Reduced von Willebrand factor-cleaving protease (ADAMTS13) activity in acute myocardial infarction. J Thromb Haemost. 2006; 4:2490–2493. [PubMed: 16898955]
23. Crawley JT, Lane DA, Woodward M, Rumley A, Lowe GD. Evidence that high von Willebrand factor and low ADAMTS-13 levels independently increase the risk of a non-fatal heart attack. J Thromb Haemost. 2008; 6:583–588. [PubMed: 18194418]
24. Zhao BQ, Chauhan AK, Canault M, Patten IS, Yang JJ, Dockal M, Scheiflinger F, Wagner DD. Von Willebrand factor-cleaving protease ADAMTS13 reduces ischemic brain injury in experimental stroke. Blood. 2009; 114:3329–34. [PubMed: 19687510]
25. de Maeyer B, De Meyer SF, Feys HB, Pareyn I, Vandeputte N, Deckmyn H, Vanhoorelbeke K. The distal carboxyterminal domains of murine ADAMTS13 influence proteolysis of platelet-decorated VWF strings in vivo. J Thromb Haemost. 2010; 8:2305–2312. [PubMed: 20695979]
26. Laje P, Shang D, Cao W, Niiya M, Endo M, Radu A, Derogatis N, Scheiflinger F, Zoltick PW, Flake AW, Zheng XL. Correction of murine ADAMTS13 deficiency by hematopoietic progenitor cell-mediated gene therapy. Blood. 2009; 113:2172–2180. [PubMed: 19141866]
27. Niiya M, Endo M, Shang D, Zoltick PW, Muvarak NE, Cao W, Jin SY, Skipwith CG, Motto DG, Flake AW, Zheng XL. Correction of ADAMTS13 deficiency by in utero gene transfer of lentiviral vector encoding ADAMTS13 genes. Mol Ther. 2009; 17:34–41. [PubMed: 18957966]
28. Gandhi C, Khan MM, Lentz SR, Chauhan AK. ADAMTS13 reduces vascular inflammation and the development of early atherosclerosis in mice. Blood. 201110.1182/blood-2011-09-376202
29. Chauhan AK, Motto DG, Lamb CB, Bergmeier W, Dockal M, Plaimauer B, Scheiflinger F, Ginsburg D, Wagner DD. Systemic antithrombotic effects of ADAMTS13. J Exp Med. 2006; 203:767–776. [PubMed: 16533881]
30. Massberg S, Brand K, Gruner S, Page S, Muller E, Muller I, Bergmeier W, Richter T, Lorenz M, Konrad I, Nieswandt B, Gawaz M. A critical role of platelet adhesion in the initiation of atherosclerotic lesion formation. J Exp Med. 2002; 196:887–896. [PubMed: 12370251]
31. Methia N, Andre P, Denis CV, Economopoulos M, Wagner DD. Localized reduction of atherosclerosis in von Willebrand factor-deficient mice. Blood. 2001; 98:14241428.
32. Gandhi C, Khan MM, Lentz SR, Chauhan AK. ADAMTS13 reduces vascular inflammation and the development of early atherosclerosis in mice. Blood. 201110.1182/blood-2011-09-376202
33. Methia N, Andre P, Denis CV, Economopoulos M, Wagner DD. Localized reduction of atherosclerosis in von Willebrand factor-deficient mice. Blood. 2001; 98:14241428.
34. Massberg S, Brand K, Gruner S, Page S, Muller E, Muller I, Bergmeier W, Richter T, Lorenz M, Konrad I, Nieswandt B, Gawaz M. A critical role of platelet adhesion in the initiation of atherosclerotic lesion formation. J Exp Med. 2002; 196:887–896. [PubMed: 12370251]
35. Sperandio M, Smith ML, Forlow SB, Olson TS, Xia L, McEver RP, Ley K. P-selectin glycoprotein ligand-1 mediates L-selectin-dependent leukocyte rolling in venules. J Exp Med. 2003; 197:1355–1363. [PubMed: 12756271]
36. Pendu R, Terraube V, Christophe OD, Gahmberg CG, de Groot PG, Lenting PJ, Denis CV. P-selectin glycoprotein ligand 1 and beta2-integrins cooperate in the adhesion of leukocytes to von Willebrand factor. Blood. 2006; 108:3746–3752. [PubMed: 16926295]
37. Lewinsohn DM, Bargatze RF, Butcher EC. Leukocyte-endothelial cell recognition: evidence of a common molecular mechanism shared by neutrophils, lymphocytes, and other leukocytes. J Immunol. 1987; 138:4313–4321. [PubMed: 3584977]
38. Tedder TF, Steeber DA, Pizcueta P. L-selectin-deficient mice have impaired leukocyte recruitment into inflammatory sites. J Exp Med. 1995; 181:2259–2264. [PubMed: 7539045]

39. Huo Y, Xia L. P-selectin glycoprotein ligand-1 plays a crucial role in the selective recruitment of leukocytes into the atherosclerotic arterial wall. Trends Cardiovasc Med. 2009; 19:140–145. [PubMed: 19818951]

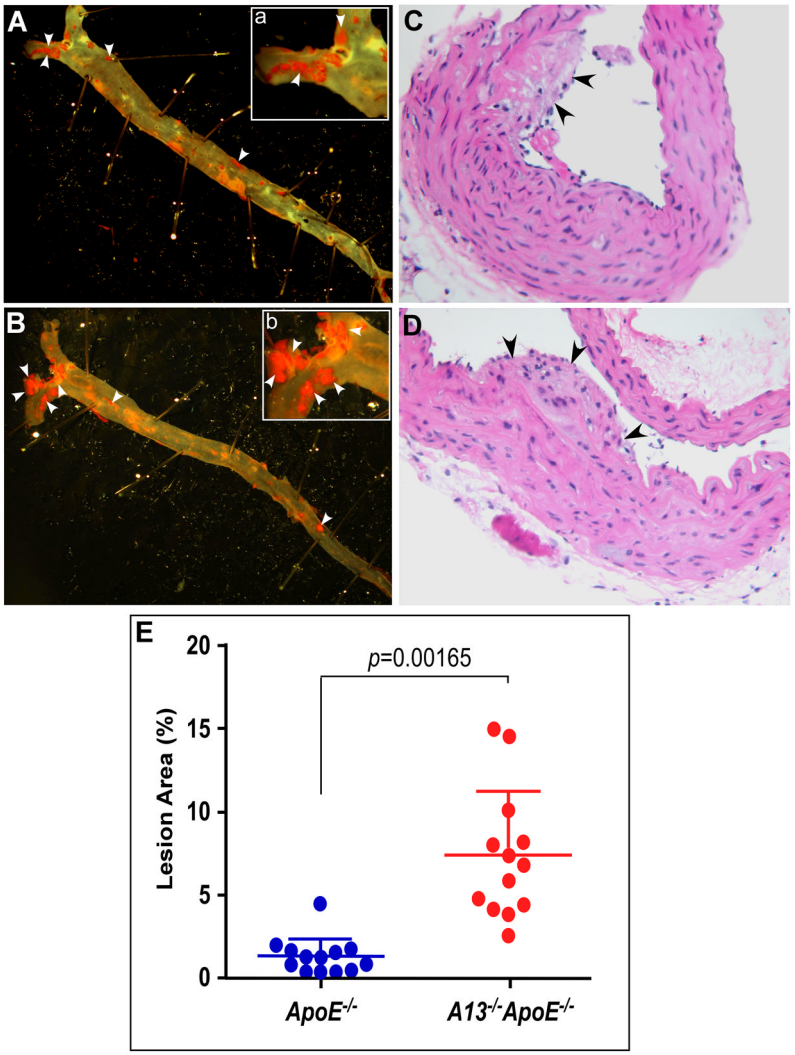

Fig. 1. Atherosclerotic lesions in the entire aorta

ApoE$^{-/-}$ (**A** and **C**) or *Adamts13*$^{-/}$*ApoE*$^{-/-}$ (**B** and **D**) mice at the age of 4 weeks were fed with a Western high fat diet for 12 weeks. The mice (n=13, in each group) were sacrificed and the entire aorta was isolated, fixed, and stained with oil red (**A** and **B**). In addition, the aorta were sectioned after paraffin embedding and stained with H&E (**C** and **D**) (200x and 400x). Digital images were obtained under a light microscope with magnifications of 100x (**A** and **B**) or 200x (**A**-a and B-b). **E**. The relative area of atherosclerotic plaques to the entire aorta with *en face* method was quantified with ImageJ software. Long and short lines across the dots in both groups represent the means and standard deviation, respectively. Student t-test was used to determine the significance between the two groups. A p value <0.01 is considered to be statistically highly significant. Arrows indicate the areas of atherosclerotic lesions.

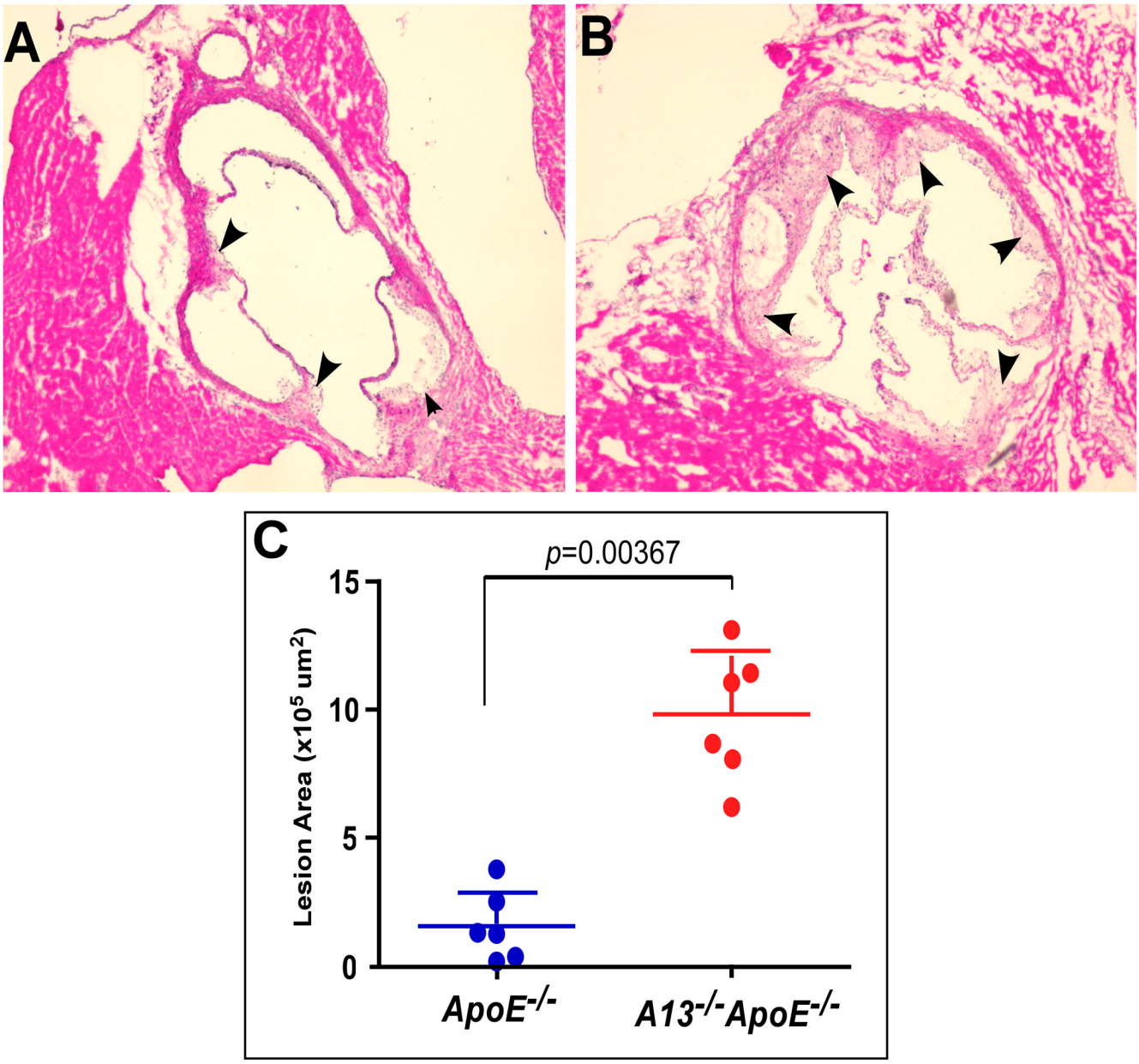

Fig. 2. Histological examination of atherosclerotic lesions in the aortic roots

ApoE$^{-/-}$ (**A**) and *Adamts13*$^{-/-}$ *ApoE*$^{-/-}$ (**B**) mice were sacrificed after 12 weeks on a high fat Western diet. Hearts were fixed with 10% neutral buffered formalin and embedded into tissue freezing medium. A series of sections (6 μm each, spaced by 80 μm) across the aortic roots were prepared using cryostat and stained with H&E. Images were obtained under light microscope at 200x. ImageJ software was used to quantify the areas of atherosclerotic lesions in all sections (arrowheads indicated). The long and short lines represent the means and standard deviation (n=6 mice, in each group) (**C**). Student *t*-test was used to determine the significance of the difference between the two groups. A *p* value <0.01 is considered to be statistically highly significant.

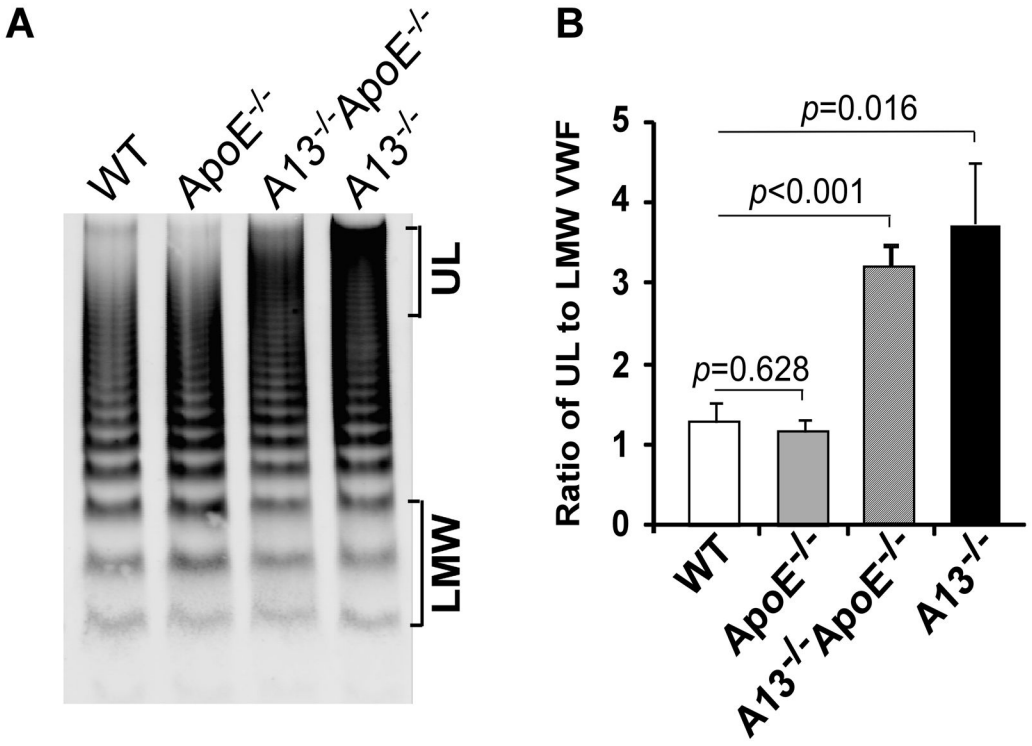

Fig. 3. Plasma VWF multimer distribution in various mice

A. Plasma VWF multimers from wild type (*WT*), *ApoE*$^{-/-}$, *A13*$^{-/-}$ *ApoE*$^{-/-}$, and *A13*$^{-/-}$ mice were determined using agarose (1%) gel electrophoresis and Western blotting as described in the Methods. **B.** ImageJ software was used to determine the ratio of ultra large (UL) to low molecular weight (LMW) VWF multimers as indicated in the right side of the image in A from various groups of mice (n=5 in each group). The *p* values less than 0.05 and 0.01 are considered to be statistically significant and highly significant, respectively.

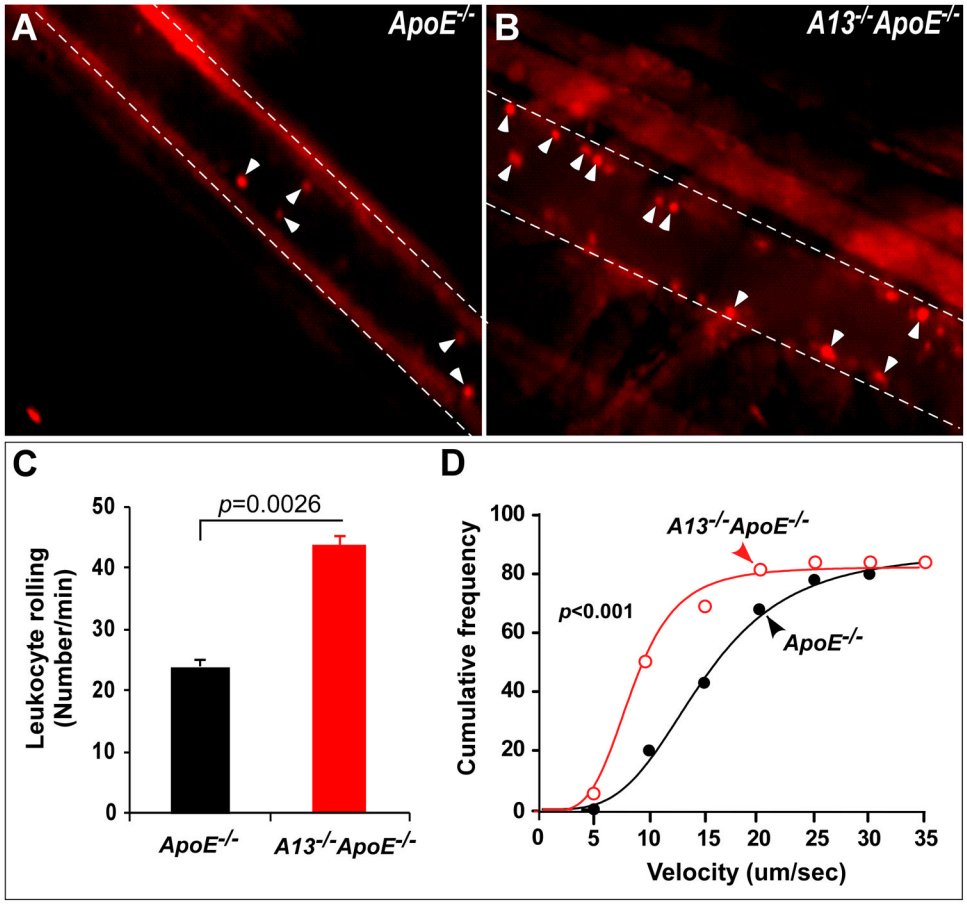

Fig. 4. Leukocyte rolling and adhesion on cremaster venules after oxidative injury

Cremaster venules of *ApoE*$^{-/-}$ and *Adamts13*$^{-/-}$ *ApoE*$^{-/-}$ mice were exposed after being anesthetized. The venules were injured by topical application of a filter paper soaked with 2.5% of $FeCl_3$. Fluorescein-labeled leukocytes rolling over the injured vessel walls were imaged in real time under an inverted fluorescent microscope. Snap shots of adhered leukocytes in *ApoE*$^{-/-}$ (**A**) and *Adamts13*$^{-/-}$ *ApoE*$^{-/-}$ mice (**B**) are shown. The numbers of leukocytes rolling over the injured vessel wall per minute (cells/min) (**C**) and the cumulated frequencies of leukocyte rolling at various velocities (μm/sec) (**D**) were determined using the NIS Elements software. The data shown in **C** are the means and standard error from 6 mice in each group (5 different sites in each mouse). Statistical analysis was performed by the Student t-test (**C**) and one-way ANOVA variance analysis (**D**), respectively. The *p* values <0.01 are considered to be statistically highly significant.

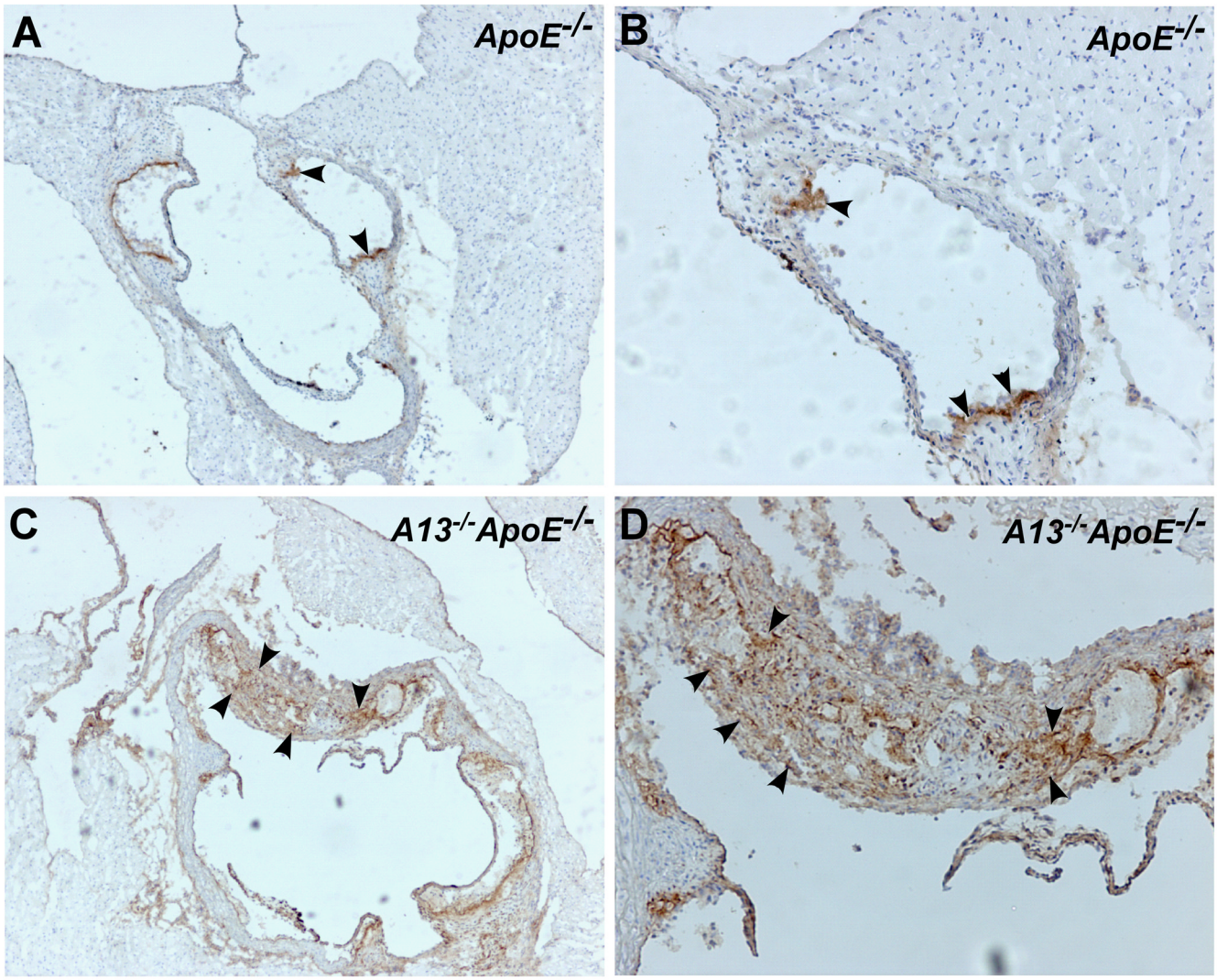

Fig. 5. Immunoperoxidase staining for macrophages in aortic arch sections

Aortic arch sections from the hearts of ApoE$^{-/-}$ mice (**A** and **B**) and the Adamts13$^{-/-}$ ApoE$^{-/-}$ mice (**C** and **D**) were stained with rat anti-mouse Mac-3 IgG, followed by biotin-labeled antirat IgG and ABC reagents as described in the Methods. Digital images were obtained under a light microscope with magnification of 400x (**A** and **C**) and 1,000x (**B** and **D**). Brown staining (arrowheads) indicates Mac-3 positive macrophages.

Table 1

Plasma levels of total cholesterol, HDL, triglyceride, and non-HDL in *ApoE*$^{-/-}$ and *Adamts13*$^{-/-}$*ApoE*$^{-/-}$ mice

	***ApoE*$^{-/-}$ (mg/dl)(n=13)**	***A13*$^{-/-}$*ApoE*$^{-/-}$(mg/dl)(n=13)**	***p* values**
Total Cholesterol	1,204.4± 397.7	1,448.1 ± 536.6	0.20
HDL	65.6 ± 17.4	95.3 ± 39.0	0.02 *
Triglyceride	123.4 ± 65.6	118.4 ± 62.3	0.84
Non-HDL	1,138.7 ± 393.3	1,352.8 ± 518.6	0.25

A13$^{-/-}$, *Adamts13*$^{-/-}$; *p* values were obtained by Student t-test (two-tailed and two samples with equal variance); n, number of mice in each group;

* *p* value<0.05 is considered to be statistically significant.